Available online at www.sciencedirect.com
SCIENCE DIRECT
Journal of Non-Crystalline Solids 352 (2006) 1832–1836
JOURNAL OF NON-CRYSTALLINE SOLIDS
www.elsevier.com/locate/jnoncrysol

Characterization of a thick layer a-Si:H pixel detector with TFA technology using a scanning electron microscope

M. Despeisse [a,*], S. Saramad [a,*], C. Ballif [b], S. Dunand [b], P. Jarron [a,*], J. Morse [c], I. Snigireva [c], C. Miazza [b], D. Moraes [a], G. Anelli [a], A. Shah [b], N. Wyrsch [b]

[a] *CERN, Department of Microelectronics, CH-1211 Geneva 23, Switzerland*
[b] *IMT, Rue A.-L. Breguet 2, CH-2000 Neuchatel, Switzerland*
[c] *ESRF – Polygone Scientifique Louis Néel-6, rue Jules Horowitz, 38000 Grenoble, France*

Available online 24 April 2006

Abstract

The electron beam induced current (EBIC) technique was used to characterize a 32 μm thick hydrogenated amorphous silicon n–i–p diode deposited on top of an ASIC, containing several channels of active feedback pre-amplifiers (AFP) with peaking time of 5 ns. The homogeneity of the sample together with the edge effects induced by the unevenness of the ASIC substrate were studied with low doses of 10–30 keV electron beam. The degradation of a-Si:H pixel detectors was measured with intense electron beam. Their charge collection and transient time were characterized with a 660 nm pulsed laser before and after the thermal annealing. All the diodes show approximately a full recovery of charge collection after thermal annealing.

PACS: 73.61.Jc; 61.43.Dq; 29.40.Wk; 61.82.Fk

Keywords: Amorphous semiconductors; Detectors; Radiation; SEM; EBIC; ASIC

1. Introduction

Electron beam induced current (EBIC) is a powerful semiconductor analysis technique [1,2], which employs a 10–30 keV electron beam from a scanning electron microscope (SEM) to scan the detector active area, and inducing a signal on the pixels' electrodes. This signal can be directly readout or can be feedback to the SEM system in such a way that any change in the generation, drift or recombination of the generated carriers in the detector is displayed as variations of contrast in EBIC images. EBIC imaging is very sensitive to electron–hole recombination, so the EBIC analysis is very useful in finding defects such as voids, crystallographic imperfections, dislocations and grain boundaries.

The EBIC method has a high potential for the characterization of n–i–p hydrogenated amorphous silicon (a-Si:H) diodes on application specified integrated circuit (ASIC) [3], as it can also be used to study the electric field in the depletion region and the degradation of a-Si:H with high doses of electrons [4]. The EBIC signal depends primarily on the strength of the electric field, so for a given potential across a junction, high dopant conditions result in narrow depletion region and higher electric field, which can be used to study the doping homogeneity. It must be noted that in addition to electric field strength, the relative dimension of depletion region compared to generation volume is also an important factor in EBIC collection efficiency. This is the reason why it is valuable to understand the basic device structure in order to interpret the results correctly.

In this work, we tried to study the homogeneity of the active area and the effects of the unevenness of the ASIC substrate, which may induce regions with high electric field. This can also explain the high leakage currents that we

* Corresponding authors. Tel.: +41 22 767 2130; fax: +41 22 767 3394.
E-mail addresses: matthieu.despeisse@cern.ch (M. Despeisse), shahyar.saramad@cern.ch (S. Saramad).

0022-3093/$ - see front matter © 2006 Elsevier B.V. All rights reserved.
doi:10.1016/j.jnoncrysol.2005.12.054

have measured in previous works on different TFA detectors [3].

2. Experimental technique

EBIC measurements and 660 nm pulsed laser tests have been performed on a TFA detector made of a 32 μm thick n–i–p a-Si:H diode deposited on an AFP ASIC [5,6]. The tested sample is presented in Fig. 1, with a schematic of the cross section, showing the ASIC passivation layer steps that induce the unevenness of the a-Si:H detector. Four 94 μm × 68 μm pixels were readout during the measurements, which were performed with the electron beam of a scanning electron microscope (SEM) at the European synchrotron radiation facility (ESRF) in Grenoble. The scanning speed and also the surface of the scan are tunable parameters. The electrons energy can be varied from 4 keV to 30 keV, but no EBIC signal was observed below 6 keV.

The electron–hole pairs generated by electron beam exhibits a maximum at a detector depth that is an increasing function of electron energy, so higher electron energy corresponds to probing deeper points of the structure. The detector reversed bias was also changed during the tests from 80 V to 280 V with three different biases of AFP, to achieve the best linearity and timing response.

In case of large beam currents and low electric fields regions, the injected charge can contribute to building of an additional internal electric field, which can modify the charge collection. For checking this condition the intensity of the electron beam was changed from 386 pA to 6189 pA, but because of non-linear relation between the measured EBIC current and the beam current for high intensities, only the lower densities were selected for the study.

The number of metastable defects created depends on electron dose, i.e. on the product of the electron intensity and the irradiation time. By using lower intensities of electron beam (~386 pA) in a short period of time (~ few seconds), damaging of the sample and modification of its electronic properties during the experiment can be neglected. On the other hand, in order to study the degradation of the sample, the TFA detector was also exposed to high doses of electron beam and the EBIC images were compared to non-irradiated ones.

The transient time and the charge collection of the irradiated and non-irradiated pixels with different bias voltages were extracted by applying a 660 nm laser pulse (2 ns pulse width). By the same method, the annealing behavior of different pixels with different irradiation dose is studied at 100 °C.

3. Experimental results

The SEM and EBIC images of two pixels of the TFA detector under study (Fig. 1) are displayed in Fig. 2. These images were taken using a 20 keV electron beam with an intensity of 386 pA and using a 150 V reverse bias on the detector. The SEM image shows a non-flatness of the deposited a-Si:H detector on each pixel edges and some pronounced geometrical effects at the pixels' corners. The EBIC image clearly shows the effect of this particular geometry on the detector electric field: higher EBIC currents are observed at the edges and the corners. Some voids can be observed in EBIC images, with darker color. Small holes with black color in the SEM image are lighter in EBIC images, because of higher electric field in these regions. The dust on the surface of the sample also shows itself as a dark spot in the EBIC image. By increasing the

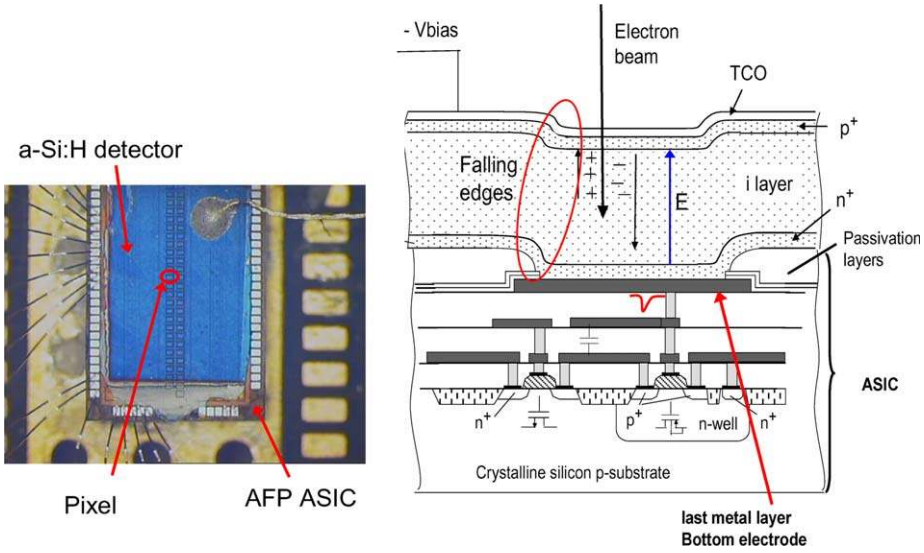

Fig. 1. (Left) Picture of the tested TFA detector: a 32 μm thick a-Si:H n–i–p diode is deposited on top of an AFP ASIC. (Right) Schematic cross section of a pixel: passivation layers are deposited on top of the last metal layer of the ASIC, and opened on top of the metal pad defining the pixel bottom electrode. The passivation layer induces a step of about 5 μm rendering the ASIC surface uneven.

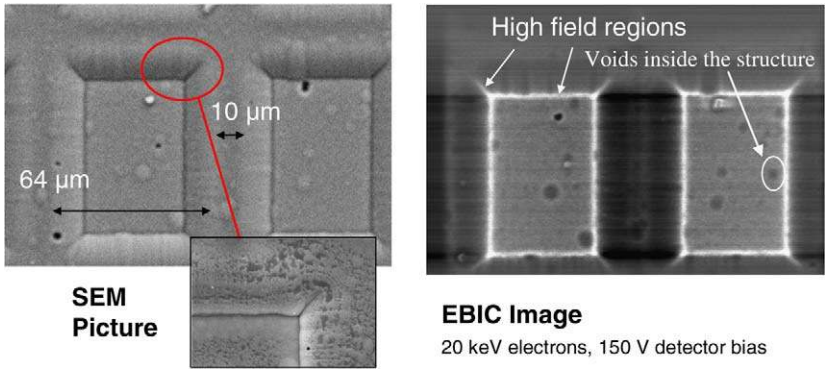

Fig. 2. (Left) Picture of two pixels taken with the SEM. On the pixel edges the passivation falling edge can be observed, a zoom in a pixel corner shows a fissure at the three different edges gathering. (Right) EBIC image of the two pixels. High field regions can be seen at the pixel edges and corners.

energy of electron beam in EBIC mode it is also possible to study the sub-surface damages that are not visible with any other technique. In Fig. 2, there is a gray spot visible in the EBIC image, which is not seen in SEM. This spot can be related to voids inside the structure.

To study the EBIC induced current, a line scan has been performed using 20 keV electron beam with an intensity of 386 pA and for 80 V, 160 V and 240 V detector reverse biases (Fig. 3). Four different regions are recognized in the output voltage of Fig. 3:

(1) A flat signal above the metal pad, which is proportional to the reverse bias voltage. This behavior is reasonable because the EBIC signal is proportional to electric field.
(2) A large peak at the beginning of the rising slope on top of the structure (p^+ a-Si:H) and above the metal pad, which corresponds to higher electric field at the edges.
(3) In the rising slope above the metal pad, the signal is decreased very fast. In this region, the electric field is perpendicular to the rising slope, so the transverse field will push the generated electrons inside the depletion region toward the rear metal pad, while the lateral one pushes them toward the region with 5 μm passivation. In this region, most of the electrons are reabsorbed through recombination processes.
(4) By passing from the end of rising slope, the electric field will push the electrons toward the rear metal contact, which increases the amplitude of the EBIC signal. Finally, in the regions far enough, for which the lateral electric field is decreased and recombination is more important, the EBIC signal completely disappeared. So it must be mentioned that because of the complex profile of the electric field, it is possible that EBIC signals are detected in the regions that are not expected.

Fig. 4 shows the EBIC images of a partly degraded pixel diode with electron beam. Two different areas of the pixel have been exposed to 386 pA and 1307 pA electron beam for ~10 min. The electron beam was then scanning back the whole pixel area, creating the EBIC image of Fig. 4. The zone irradiated with a low intensity beam shows a dar-

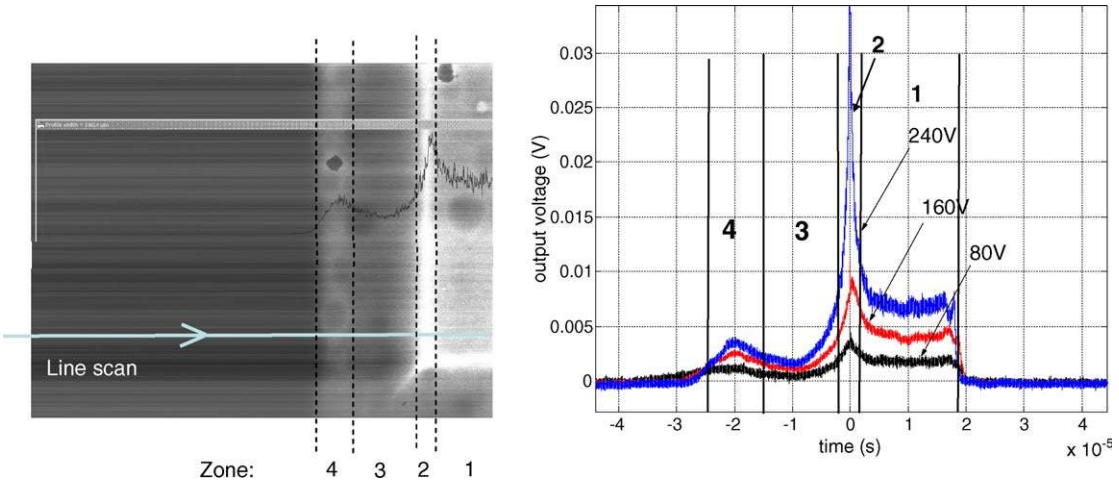

Fig. 3. (Left) EBIC image of a pixel's corner and line scan representation. (Right) Signal shape for a line scan of 20 keV electron beam, for three different detector biases (80 V, 160 V and 240 V). A model with four different 'zones' is extracted.

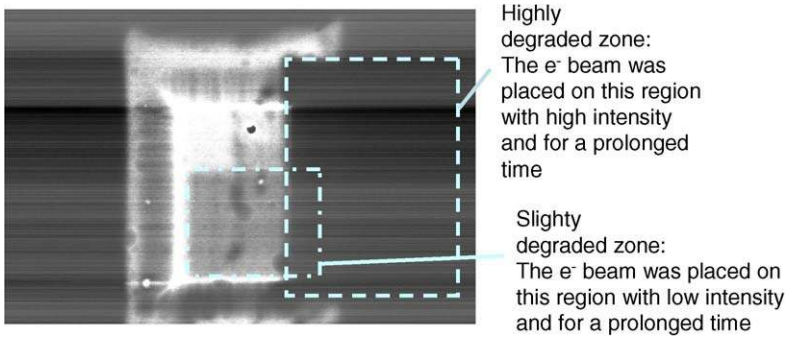

Fig. 4. EBIC Image of a pixel. The e^- beam was first focused on a specified area of the pixel with low intensity, leading to a slight degradation. The beam was then focused on a second area but with high intensity, leading to a high degradation of the diode.

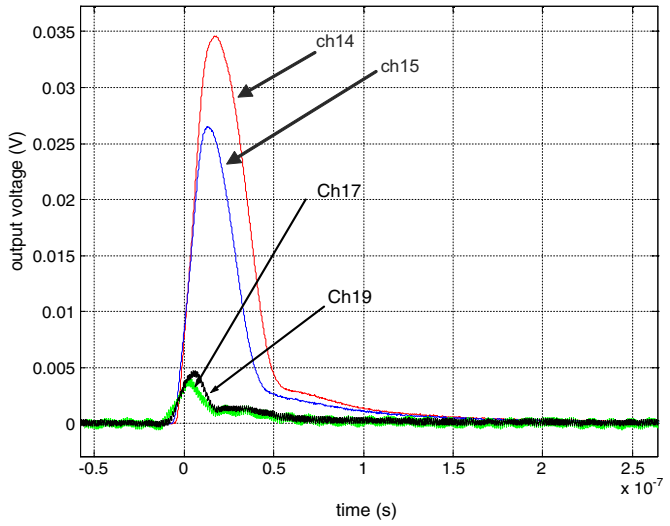

Fig. 5. Current transient response of irradiated (ch15, ch17 and ch19) and non-irradiated pixels (ch14) tested with 660 nm pulsed laser.

ker contrast compared to the non-irradiated part of the pixel, while the area irradiated with high intensity beam appears totally black, indicating a strong degradation of the diode performance. To study the charge collection of the degraded pixels, three irradiated pixels and a non-radiated one, which is taken as a reference, were tested with 660 nm pulsed laser (Fig. 5). This technique was also used before EBIC measurements to characterize the detector charge collection speed for steady state detector biases [7]. Two of the degraded pixels (ch17, ch19) had a charge collection equal to 10% of the reference pixel (ch14). The pixel ch15 was less degraded during the test. Finally, the pixel ch18, which was exposed to 26 keV electrons at an intensity of $\sim 5 \times 10^{16}$ electrons/cm^2, had an estimated charge collection of about 1% of the charge collected in ch14 (Since no signal was observed for the test condition of Fig. 5, this measurement has been done with higher intensity of laser beam). After 15 h of annealing at 100 °C and under 150 V reverse bias, ch17, ch19 returned back to a charge collection corresponding to 90% of ch14 and for the ch18 after 21 h annealing at the same temperature and the same bias voltage, the charge collection is recovered to 85% of the ch14.

By comparing the current transient response of the irradiated and non-irradiated pixels, it is clear that the more degraded pixels have the lower charge collection but the charge transit time for most of the carriers is smaller. This can be explained by the fact that the irradiated pixels have a higher dangling bond density, so the depletion region is smaller for the same bias voltage and we have higher electric field in that region. On the other hand, the induced defects can trap the generated carriers and decrease the amplitude of the signal, but more detail calculation will show that even for ch17 the mean free path of the electrons is about 9 times of depletion thickness, so the trapping can be neglected [8].

4. Conclusion

Our experimental results show that EBIC technique is a powerful tool for studying the surface and sub-surface defects, electric field profile and also the homogeneity of the TFA detectors. Even by simulation the EBIC current, it is possible to extract internal collection efficiency with accuracy depending on the accuracy of the EBIC gain measurements. High field regions have been observed at the pixel edges and corners, which explain the higher leakage currents measured on a-Si:H diodes deposited on ASIC compared to diodes deposited on a glass substrate.

Metastable defects can be formed in hydrogenated amorphous silicon detector by ionizing particles, such as low energy electrons, but the experimental results show the possibility of almost full recovery of charge collection after thermal annealing. This radiation hardness can make these detectors a good candidate for future high-energy physics experiments.

References

[1] H.J. Leamy, J. Appl. Phys. 53 (1982) R51.
[2] S. Zhu, E.I. Rau, F.H. Yang, Semicond. Sci. Technol. 18 (4) (2003) 361.

[3] N. Wyrsch, C. Miazza, S. Dunand, A. Shah, G. Anelli, M. Despeisse, P. Jarron, J. Kaplon, D. Moraes, A. Garrigos Sirvent, G. Dissertori, G. Viertel, Phys. Stat. Solidi C 1 (5) (2004) 1284.
[4] A. Yelon, H. Fritzsche, H.M. Branz, J. Non-Cryst. Solids 266–269 (2000) 437.
[5] G. Anelli, K. Borer, L. Casagrande, M. Despeisse, P. Jarron, N. Pelloux, S. Saramad, Nucl. Instrum. Methods A 512 (2003) 117.
[6] D. Moraes, G. Anelli, M. Despeisse, G. Dissertori, A. Garrigos, P. Jarron, J. Kaplan, C. Miazza, A. Shah, G. Viertel, N. Wyrsch, J. Non-Cryst. Solids 338–340 (2004) 729.
[7] M. Despeisse, G. Anelli, S. Commichau, G. Dissertori, A. Garrigos, P. Jarron, C. Miazza, D. Moraes, A. Shah, N. Wyrsch, G. Viertel, Nucl. Instrum. Methods Phys. Res. A 518 (2004) 357.
[8] S. Saramad, P. Jarron, M. Despeisse, D. Moraes, G. Anelli, J. Kaplon, Presented at Seventh International Conference on Large Scale Applications and Radiation Hardness of Semiconductor Detectors, Florence, Italy, October 5–7, 2005.